



DOI: doi.org/10.21009/SPEKTRA.051.02

# THE DETERMINATION OF BARIUM STRONTIUM TITANATE THIN FILM BAND GAP ENERGY $Ba_{0,15}Sr_{0,85}TiO_3$ USING ULTRAVIOLET-VISIBLE SPECTROSCOPY

Rahmi Dewi\*, Krisman, Zulkarnaen, Rahmi Afrida Syahraini,  
TS Luqman Husein

*Physics Department, Math and Science Faculty, Universitas Riau, Pekanbaru, 28293, Indonesia*

\*Corresponding Author Email: drahmi2002@yahoo.com

**Received:** 28 March 2020

**Revised:** 1 April 2020

**Accepted:** 4 April 2020

**Online:** 26 April 2020

**Published:** 30 April 2020

**SPEKTRA:** Jurnal Fisika dan  
Aplikasinya

p-ISSN: 2541-3384

e-ISSN: 2541-3392



## ABSTRACT

A thin layer of Barium Strontium Titanate  $Ba_{0,15}Sr_{0,85}TiO_3$  (BST) was developed on a glass substrate using a sol-gel method with annealing temperatures and spin coating process at 3500 rpm for 30 seconds. The annealing temperature varied from 600°C, 650°C, and 700°C. Characterization of optical properties was developed using UV-Vis spectroscopy to determine the energy bandgap. The values of the BST thin layer energy band at the annealing temperature were 3.55 eV, 3.32 eV, and 3.10 eV, respectively. The results indicate that the BST thin film was a semiconductor material.

**Keywords:** the thin layer of barium strontium titanate, sol-gel method, optical characterization, the energy bandgap

## INTRODUCTION

Science and technology as a necessity in human life influence various fields of life and become a criterion for the progress of a country. Technological advancements are indicated by an increase in the need for electronic devices [1]. The production of these electronic devices requires better quality materials [2]. It drives many researchers to study the materials that can be used as the raw materials for electronic devices. The various applications, such as the use of FRAM (*Ferroelectric Random Access Memory*), manufacturing thin-film capacitors, pyroelectric sensors due to temperature changes, pressure sensors (*piezoelectric*), a light sensor was utilizing the semiconductor connection properties, and *optoelectronics* [3,4].

Ferroelectric material, which is currently being developed, is Barium Strontium Titanate (BST). BST thin film is a ferroelectric material formed of Barium Titanate ( $\text{BaTiO}_3$ ), which is doped with strontium (Sr). Propagation is carried out to increase the dielectric constant and to reduce dielectric loss at low frequencies [5].

Barium Strontium Titanate (BST) is a ferroelectric material that is widely applied for storage media and has a perovskite crystal structure. Some researchers believe that BST has the potential to replace the thin layer of  $\text{SiO}_2$  in the Metal Oxide Semiconductor (MOS) circuit. Until now, the results of studies on BST films usually have dielectric constants, which are lower than the bulk form. The suitable grain microstructure, oxygen vacuum, interfacial layer formation, and oxidation of the bottom electrode or Si, are believed to be factors decreasing in electrical properties [6].

The preparation methods which are often used in the synthesis of layered and porous nanomaterials are the sol-gel, intercalation, and inclusion methods. The sol-gel method is a method of preparing solids with a low-temperature technique that involves the transition from a system with microscopic particles dispersed in a liquid (sol) to a macroscopic material (gel) containing liquid. When the liquid evaporates, it remains a hard material like glass. Sol-gel is an amorphous material and does not have uniform pore dimensions. Sol-gel synthesis generally goes through the stages of hydrolysis and condensation [7].

BST thin layer in this study was made by the sol-gel method or known as the Chemical Solution Deposition (CSD) method, by using a chemical solution on a substrate processed by the spin coating technique. The sol-gel method has the advantage of a simple process, and it can be done at room temperature, short fabrication cycles, high purity, the cost required is relatively inexpensive, and can control the stoichiometry layer well [8]. Where  $x$  is a percentage number for Ba and Sr in  $\text{Ba}_{1-x}\text{Sr}_x\text{TiO}_3$ , and Ti is for 100%. The ratio of Ba and Sr is 15% : 85%. The thin layer was characterized using Ultraviolet-Visible (UV-Vis) spectroscopy to determine the optical properties and the gap energy using the Tauc Plot method.

The energy band gap is a gap located between the valence band and the conduction band, where electrons will jump from one band to the other. This gap will show the nature of a solid, whether it is a conductor, an insulator, or a semiconductor. The gap energy is the minimum needed to excite electrons from the valence band to the conduction band. When a semiconductor is charged with energy corresponding to the bandgap energy, the electron will

be excited into the conduction band, leaving a positive charge called a hole. Energy band gap control is performed to obtain the energy needed to excite electrons or holes in the material or energy emitted by electrons or holes when returning to the ground state can be modified as needed [9].

The known value of the energy band is important to find out how much energy is needed to excite the electrons from the valence band to the conduction band so that a good application for this material can be determined. Energy bands that are too small will cause electron jumps from the valence band to the conduction band so that the electrons are less free, while energy bands that are too large will inhibit electron jumps so that the flow of electrons will be impeded [10].

## METHOD

The manufacturing of a thin layer  $\text{Ba}_{0.15}\text{Sr}_{0.85}\text{TiO}_3$  uses the Sol-gel method. While sample characterization uses UV-Vis spectroscopy. The raw materials needed for the sample included *Barium Carbonate* ( $\text{BaCO}_3$ ), *Strontium Carbonate* ( $\text{SrCO}_3$ ), and *Titanium Isopropoxide* solution ( $\text{Ti}(\text{OC}_3\text{H}_7)_4$ ). The manufacturing processes of BST thin films using the sol-gel method are as follows: Strontium Carbonate ( $\text{SrCO}_3$ ) and Barium Carbonate ( $\text{BaCO}_3$ ) are put into glass bottles. A 16 ml Acetyl Acid solution was added. The solution is stirred with a magnetic stirrer on a hotplate until it is clear for  $\pm 1$  hour. 1 ml of titanium isopropoxide  $\text{Ti}(\text{OC}_3\text{H}_7)_4$  was added to the solution while stirring for  $\pm 1$  hour. The acetyl solution was dropped into a solution of 3 drops while constantly stirring on the hotplate until the solution was yellowish clear ( $\pm 1$  hour).

$\text{Ba}_{0.15}\text{Sr}_{0.85}\text{TiO}_3$  solution are grown on a glass substrate by spin coating at a speed of 3500 rpm for 30 seconds. Then the sample is heated at  $150^\circ\text{C}$  for 30 minutes in the oven. The next process is to strengthen the bonds of atoms and remove substances that are not needed, usually at temperatures of  $300^\circ\text{C}$  to  $400^\circ\text{C}$ . In this study, the samples were pretreated at  $300^\circ\text{C}$  for 30 minutes in the furnace. Then the samples were annealed at temperatures varying to  $600^\circ\text{C}$ ,  $650^\circ\text{C}$ , and  $700^\circ\text{C}$  for 1 hour.

The flow diagram of sample manufacturing can be seen in FIGURE 1 below.

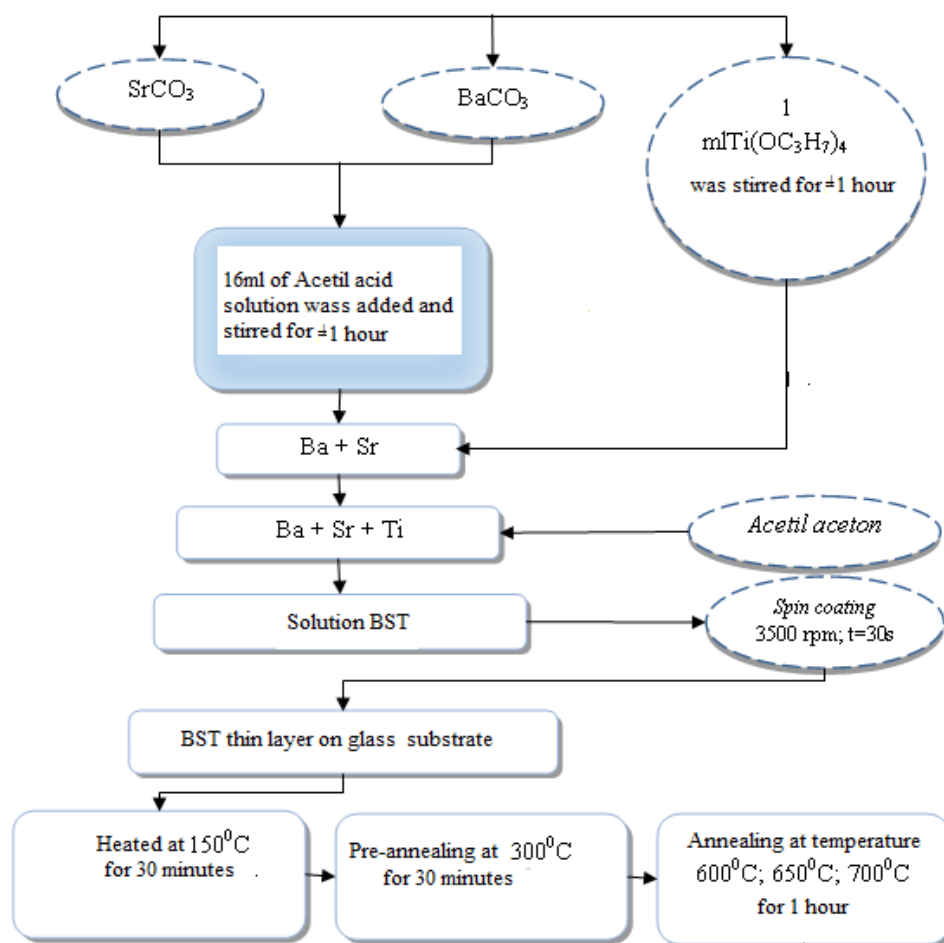


FIGURE 1. The flow diagram of sample manufacturing.

The determination of the optical band gap in thin films can be done by processing the transmittance data, which was obtained from characterization using Ultraviolet-Visible spectroscopy. Wavelengths that used for measurement of transmittance are from ultraviolet light to visible light (300 nm to 800 nm). The value of the refractive index and thickness of the thin layer is determined using the following equation [11]:

$$N = 2 n_s \frac{T_M - T_m}{T_M T_m} + \frac{n_s^2 + 1}{2} \quad (1)$$

$$n = \sqrt{N + \sqrt{N^2 - n_s^2}} \quad (2)$$

Thin layer thickness values can be determined from the results of the calculation of the refractive index value using the following equation:

$$d = \frac{\lambda_1 \lambda_2}{2(\lambda_1 n_2 - \lambda_2 n_1)} \quad (3)$$

The calculation result of thin-film thickness is then used to determine the coefficient of absorption of the thin layer for each wavelength using the following equation:

$$\alpha = -\frac{1}{d} \ln(T) \quad (4)$$

The absorption coefficient of the thin layer has been obtained, then determine  $h\nu$  where  $h\nu = h \frac{c}{\lambda}$ . Then determine the optical band gap using the Tauc plot method, which is the method of determining the optical band gap by extrapolating from the relationship graph  $(h\nu)$  as abscissa and  $(ah\nu)^n$  as a coordinate to cut the energy axis and from the curve can be determined the gap energy value of each material  $Ba_{1-x}Sr_xTiO_3$  which was examined. The value of  $(ah\nu)^n$ ,  $n = 1/2$  for the direct transition process and  $n = 2$  for the indirect transition process [12].

## RESULT AND DISCUSSION

Absorbance values are obtained from the results of characterization using UV-Vis spectroscopy.

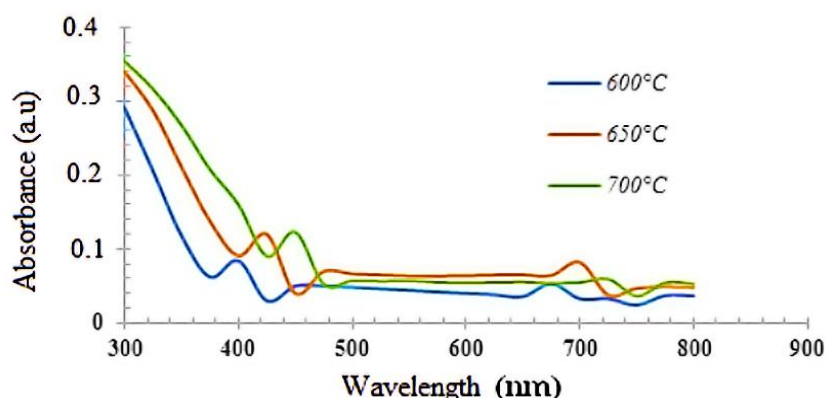


**FIGURE 2.** The thin layer absorbance spectrum  $Ba_{0.15}Sr_{0.85}TiO_3$  at temperature annealing 600°C, 650°C and 700°C.

FIGURE 2 shows the absorbance spectrum of  $Ba_{0.15}Sr_{0.85}TiO_3$  thin-layer with temperature variations of 600°C, 650°C, and 700°C. The results of the characterization of  $Ba_{0.15}Sr_{0.85}TiO_3$  thin films at 600°C annealing temperature obtained the highest absorbance value of 0.29113 a.u. The highest absorbance value at 650°C annealing temperature was 0.33977 a.u., while at 700°C annealing temperature, the highest absorbance value was 0.35411 a.u. The absorbance value of  $Ba_{0.15}Sr_{0.85}TiO_3$  thin film in the ultraviolet region increases with increasing annealing temperature given in the sample, as shown in FIGURE 2. In contrast, in the visible area, the absorption occurs is small and does not experience significant differences.

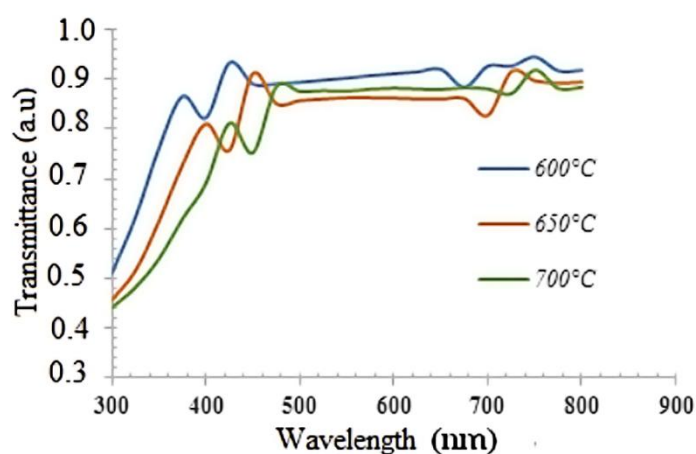


**FIGURE 3** Thin Layer Transmittance Spectrum  $Ba_{0.15}Sr_{0.85}TiO_3$  at Temperature annealing  $600^\circ C$ ,  $650^\circ C$  and  $700^\circ C$ .

FIGURE 3 shows the transmittance spectrum of  $Ba_{0.15}Sr_{0.85}TiO_3$  thin films with annealing temperature variation of  $600^\circ C$ ,  $650^\circ C$ , and  $700^\circ C$ . Based on FIGURE 3, the maximum transmittance values are  $T_{M1}$  0.94527 and  $T_{M2}$  0.93351, minimum transmittance  $T_{m1}$  0.82269, and  $T_{m2}$  0.88436 with wavelengths  $\lambda_1$  750 nm and  $\lambda_2$  425 nm for annealing temperatures of  $600^\circ C$ . At annealing temperature of  $650^\circ C$ , the maximum transmittance value is obtained, namely  $T_{M1}$  0.91626 and  $T_{M2}$  0.91186, minimum transmittance  $T_{m1}$  0.75794 and  $T_{m2}$  0.82731 with wavelengths  $\lambda_1$  725 nm and  $\lambda_2$  450 nm, while samples given annealing temperature  $700^\circ C$  has a maximum transmittance value that is equal to  $T_{M1}$  0.91892 and  $T_{M2}$  0.88591, minimum transmittance  $T_{m1}$  0.75274 and  $T_{m2}$  0.87154 with wavelengths  $\lambda_1$  750 nm and  $\lambda_2$  475 nm.

Transmittance at  $Ba_{0.15}Sr_{0.85}TiO_3$  thin film occurs in the increase of transmittance value at wavelengths of 300-450 nm. Based on the transmittance spectrum, results in the thin layer  $Ba_{0.15}Sr_{0.85}TiO_3$  shows that the higher of annealing temperature, the smaller the transmittance value. This is because the constituent atoms will become denser, resulting in collisions of light particles with the atomic constituent layers will be more frequent, so it is difficult for light to be able to pass through the layer. The higher the absorbance value, the lower the transmittance value will be. A high absorbance value means that many large particles are found in the thin film [9].

The refractive index value ( $n$ ) is obtained from the calculation results by processing the maximum transmittance data ( $T_M$ ), minimum transmittance ( $T_m$ ), and wavelength ( $\lambda$ ) using equation (2). Furthermore, by using equation (3) of the refractive index value ( $n$ ) obtained, the thickness value of each thin layer is obtained as in TABLE 1.

**TABLE 1.** The refraction index value and thin layer Ba<sub>0,15</sub>Sr<sub>0,85</sub>TiO<sub>3</sub> thickness.

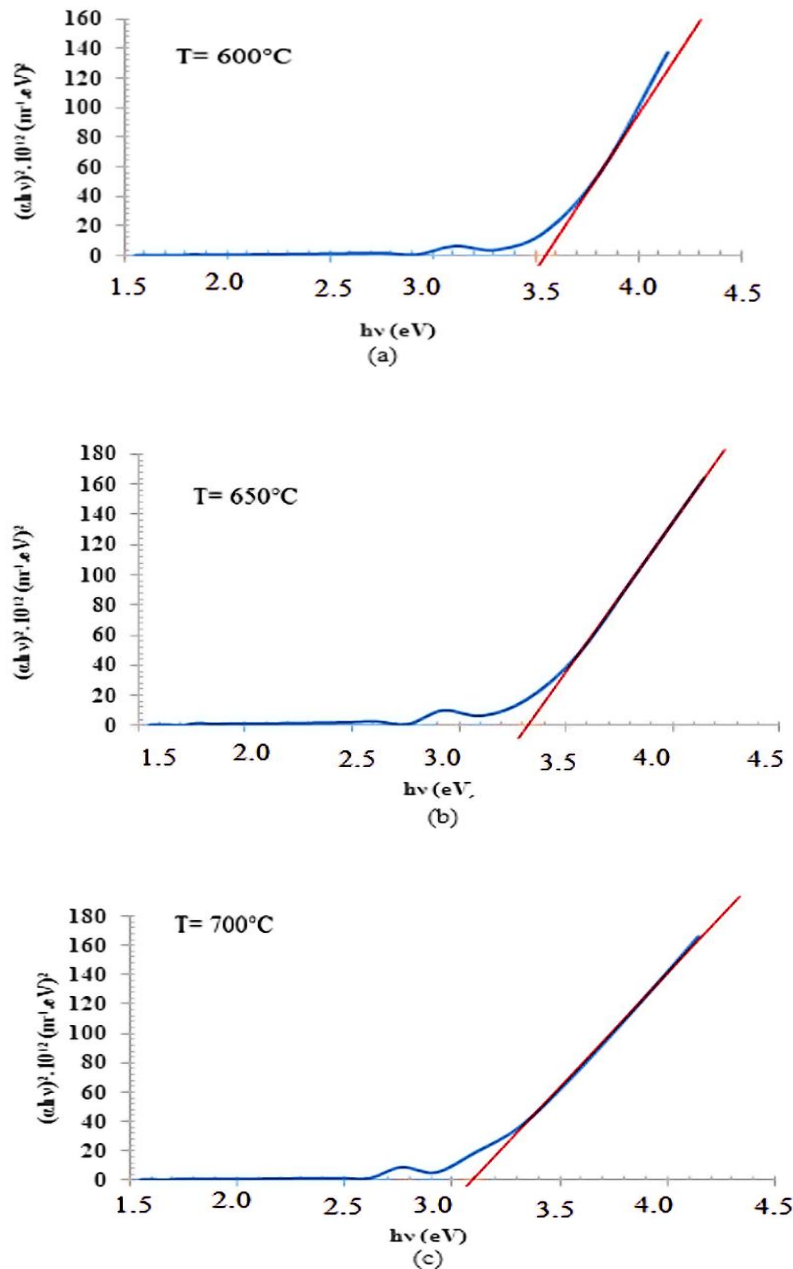
Temperature	$\lambda$ (nm)	$T_M$	$T_m$	n	d (m)
600°C	750	0.945257	0.822697	1.72	2.37 x 10 <sup>-7</sup>
	425	0.933512	0.884362	1.82	
650°C	725	0.916263	0.757949	1.81	2.53 x 10 <sup>-7</sup>
	450	0.911864	0.827313	2.01	
700°C	750	0.918925	0.752749	1.68	2.62 x 10 <sup>-7</sup>
	475	0.885911	0.871545	1.97	

TABLE 1 displays the refractive index values and thickness of Ba<sub>0,15</sub>Sr<sub>0,85</sub>TiO<sub>3</sub> layers with annealing temperature variation of 600°C, 650°C, and 700°C. The thickness of Ba<sub>0,15</sub>Sr<sub>0,85</sub>TiO<sub>3</sub> thin layer at an annealing temperature of 600°C, 650°C, and 700°C respectively amounted to 237 nm, 253 nm, and 262 nm. Layer thickness (d) increases with increasing annealing temperature. Research conducted by Yu et al. reported that on a thin layer of TiO<sub>2</sub> grown on a glass substrate by the PLD method (pulsed laser deposition method), the transmittance of the layer decreases with increasing layer thickness. By investigating the morphology of the growing layer, Yu et al. found that as the thickness of the layer increases, the diameter of the layers making up the layer also increases. The increasing diameter of the grains making up this layer results in increased surface roughness, which in turn increases the scattering of photon waves on the surface of the layer [13]. Lee et al. reported the same. for a thin layer of B<sub>2</sub>O<sub>3</sub> and Li<sub>2</sub>O (B/L)-added Ba<sub>0,6</sub>Sr<sub>0,4</sub>TiO<sub>3</sub> (BST) [14].

The magnitude of the gap energy value (energy band gap) can be obtained from extrapolating the linear relationship graph  $(\alpha hv)^2$  to the photon energy (hv). The intersection of the graph and the flat axis shows the width of the energy bandgap. The plot graph between  $(\alpha hv)^2$  and (hv) is shown in FIGURE 4 (a) (b) (c).

FIGURE 4 displays chart  $(\alpha hv)^2$  as a function hv of Ba<sub>0,1</sub>Sr<sub>0,9</sub>TiO<sub>3</sub> thin layer at annealing temperature variations. By making a line using the Tauc plot method of the value  $(\alpha hv)^2$  taking the point of intersection of the line with the photon energy on the x-axis, the gap energy value obtained at an annealing temperature of 600°C, 650°C and 700°C are 3.55 eV, 3.32 eV, respectively and 3.10 eV.

The energy gap indicates the movement of electrons across the valence band to the conduction band. From FIGURE 4, it is found that the width of the energy gap (E<sub>g</sub>) decreases with increasing annealing temperature applied to the sample. This is because small crystalline crystals shrink and are swallowed up by larger crystalline grains. The growth of this grain occurs when primary crystallization stops [15]. Higher annealing temperature causes the crystal structure to be more dense and compact, so the energy gap is smaller. The energy gap range for each sample is not too far away because the annealing temperature range used is 50°C. This indicates that if the gap width of the energy decreases, more electrons can undergo an electronic transition. Its transition from the valence band to the conduction band so that the thin layer is increasingly conductive [16].



**FIGURE 4** (a) (b) (c) Chart  $(\alpha h\nu)^2$  as the function of  $h\nu$   $\text{Ba}_{0.15}\text{Sr}_{0.85}\text{TiO}_3$  thin layer with annealing temperature variations.

Gap energy is analyzed to determine whether the material is a conductor, a semiconductor, or an insulator. Based on the gap energy values obtained in  $\text{Ba}_{0.15}\text{Sr}_{0.85}\text{TiO}_3$  thin films, the gap energy range is 3.10 eV to 3.55 eV, which states that the material in this study is a semiconductor. Material is semiconductor if it has gap energy smaller than 6 eV (1eV - 6 eV). The smaller the gap energy value, the gap of the energy band (between the conduction band

and the valence band) is smaller, so that the electrons in the conduction band more easily to jump (excitation) to the valence band [16].

## CONCLUSION

The CO gas monitoring measuring device with dimensions of 11cm x 8.6 cm x 2.9 cm using MQ-135 sensor and Arduino Uno microcontroller to display temperature and humidity on a 4.2 Inch LCD. Krisbow KD09-224 Carbon Monoxide Meter is a comparison tool or calibrator, against our monitoring gauges. Testing by experimenting as much as 15 times, to determine the value of the measurement uncertainty. Based on the results of the data, when testing, the average amount of measurement  $(\bar{X}) = 103.33$ , with a standard deviation  $\delta = 1.29$ , and the uncertainty value of the measurement results (UA\_1) is 0.33%.

## REFERENCES

- [1] M. Z. Becker, N. Shomrat and Y. Tsur, "Recent Advances in Mechanism Research and Methods for Electric-Field-Assisted Sintering of Ceramics," *Advanced Materials*, 2018, vol. 30, no. 41.
- [2] H. Sharma *et al.*, "Surface, phase transition and impedance studies of Zr- mutated BaTiO<sub>3</sub> lead-free thin films," *Results in Physics*, 2019, vol. 13, 102190.
- [3] A.S. Everhardt *et al.*, "Temperature-independent giant dielectric response in transitional BaTiO<sub>3</sub> thin films," *Applied Physics Reviews*, 2020, vol. 7, no. 1.
- [4] R.A. Malik *et al.*, "Thermal-stability of electric field-induced strain and energy storage density in Nb-doped BNKT-ST piezoceramics," *Journal of the European Ceramic Society*, 2018, vol. 38, no. 6.
- [5] M. Zhou *et al.*, "Novel BaTiO<sub>3</sub>-based lead-free ceramic capacitors featuring high energy storage density, high power density, and excellent stability," *J. Mater. Chem. C*, 2018, vol. 6, no. 31.
- [6] M. Zhou *et al.*, "High energy storage properties of (Ni<sub>1/3</sub>Nb<sub>2/3</sub>)<sub>4+</sub>-complex-ion modified (Ba<sub>0.85</sub>Ca<sub>0.15</sub>)(Zr<sub>0.10</sub>Ti<sub>0.90</sub>)O<sub>3</sub> ceramics," *Mater. Res. Bull.*, 2017, vol. 98.
- [7] R. Dewi, "Formation and characterization of typical films Ba<sub>0.2</sub>Sr<sub>0.8</sub>TiO<sub>3</sub> using XRD, FESEM and Spectroscopy impedance," *J. Phys. Conf. Ser.*, 2018, vol. 1120, no. 1.
- [8] B. I. Edmondson *et al.*, "Epitaxial, electro-optically active barium titanate thin films on silicon by chemical solution deposition," *J. Am. Ceram. Soc.*, 2020, vol. 103, no. 2.
- [9] R. Dewi *et al.*, "Characterization of optical properties of thin-film Ba<sub>1-x</sub>Sr<sub>x</sub>TiO<sub>3</sub> (x = 0,70; x= 0,75; and x=0,80) using ultraviolet-visible spectroscopy," *AIP Conf. Proc.*, 2019, vol. 2169.
- [10] N. A. Bakar *et al.*, "Physical, electrical and optical characterizations of Ba<sub>0.5</sub>Sr<sub>0.5</sub>TiO<sub>3</sub> (BST) thin films," *2ND Int. Conf. Appl. PHOTONICS Electron*, Jan. 2019, vol. 2203.
- [11] V. Kavitha *et al.*, "Optical and structural properties of tungsten-doped barium strontium titanate," *Mater. Today Proc.*, 2019.

- [12] C. Gautam *et al.*, “Synthesis, optical and solid NMR studies of strontium titanate borosilicate glasses doped with TeO<sub>2</sub>,” *Results Phys.*, 2020, vol. 16.
- [13] S. Y. Lou *et al.*, “(1 1 0) – textured BaSn<sub>0.15</sub>Ti<sub>0.85</sub>O<sub>3</sub>/ Ba<sub>0.6</sub>Sr<sub>0.4</sub>TiO<sub>3</sub>/ BaZr<sub>0.2</sub>Ti<sub>0.8</sub>O<sub>3</sub> multilayers with enhanced tunable performance,” *J. Alloys Compd.*, Dec. 2019, vol. 781.
- [14] W. H. Lee *et al.*, “Structural and dielectric properties of B<sub>2</sub>O<sub>3</sub>/ Li<sub>2</sub>O-added Ba<sub>0.6</sub>Sr<sub>0.4</sub>TiO<sub>3</sub> multilayer ceramics for tunable devices,” *Ceram. Int.*, 2020, vol. 46, no. 3.
- [15] S. J. Gao, “Dielectric properties and synthesis of magnesium doped strontium titanate with annona squamosa-like,” *Results Phys.*, no. Dec. 2019, vol. 16.
- [16] T. Zaman *et al.*, “Mono and co-substitution of Sr<sup>2+</sup> and Ca<sup>2+</sup> on the structural, electrical, & optical properties of barium titanate ceramics,” *Ceram. Int.*, 2019, vol. 45, no. 8.